



ELSEVIER

Contents lists available at ScienceDirect

Chemical Engineering Research and Design

journal homepage: www.elsevier.com/locate/cherd

 ICChemE
 ADVANCING
 CHEMICAL
 ENGINEERING
 WORLDWIDE


An investigation on the evolution of granule formation by in-process sampling of a high shear granulator

Faiz Mahdi, Ali Hassanpour*, Frans Muller

School of Chemical and Process Engineering, University of Leeds, LS2 9JT, UK

ARTICLE INFO

Article history:

Received 28 July 2017

Received in revised form 28 October 2017

Accepted 31 October 2017

Available online 11 November 2017

Keywords:

Granulation mechanisms

Sampling system

Image-based techniques

High shear granulation

Over wetted and granule size

ABSTRACT

Understanding the growth mechanisms in granulation process is an important topic, providing valuable insights and supports control strategies. Typically, observations in high shear granulators are made after stopping the process. In this work, an in-process sampling technique is described and applied to a high shear wet granulation process. Different samples can be collected over the course of the high shear granulation process. This allowed observation of the evolution of granules during addition of water at a constant flowrate. For a typical pharmaceutical formulation, we observed that granules nucleate in the first 2 min after starting the water addition and then grow to an average size of 200–1200 μm at 12.5 min, corresponding to a sharp increase in torque. Longer water addition times lead to oversized granules and eventually a paste and highly fluctuating torque. Sampling was also continued after stopping water addition which showed with time larger formed granules smoothen, whilst the smaller ones disintegrate. The work shows the in-process sampling can facilitate the identification of the granule growth kinetics and required binder quantity in high shear granulation.

© 2017 The Authors. Published by Elsevier B.V. on behalf of Institution of Chemical Engineers. This is an open access article under the CC BY-NC-ND license (<http://creativecommons.org/licenses/by-nc-nd/4.0/>).

1. Introduction

Granulation can be carried out by a wet or dry process, depending on the properties of the primary and final products (Tardos et al., 1997). The wet granulation process is performed by spraying liquid binder onto the particles while agitated in different devices such as tumbling drum, fluidized bed or high shear mixer (Tardos et al., 1997). Wet granulation in a high shear mixer is usually achieved by shorter processing time and more effective liquid binder addition compared to other types of granulations (Augsburger and Vuppala, 1997; Hemati and Benali, 2007). Iveson et al. (2001) states that, wet granulation mechanisms can be described by wetting and nucleation, consolidation during growth and attrition with breakage. These mechanisms control the obtained granule properties. Moreover, they are influenced by a combination of formulation design (e.g. feed powder and binder properties) and process design such as type of granulator and the operating parameters.

Two methods are usually used to characterize the physical properties of the granules. Traditional non-image based methods such as pycnometry, BET analysis as well as X-ray tomography (Klobes et al., 1997; Lowell et al., 2012; Rahmanian et al., 2009; Stanley-Wood and Shubair, 1979) are implemented to characterise the structural properties of the granules. On the other hand, granule size and shape is characterised by the image-based or laser diffraction techniques (Farber et al., 2003; Garboczi, 2002; Hancock and Mullarney, 2005). Although, the image-based techniques are often costly due to operating and capital costs of equipment, it is accurate and give more information (Farber et al., 2003; Garboczi, 2002; Hancock and Mullarney, 2005).

To process most of particles in the granulation system, Tardos et al. (1997) remarked that a number of notes must be considered. A critical minimum amount of liquid binder is an important characteristic of the granulation system to ensure enough stickiness on the particle surface. This note will be studied in further details in this research. Furthermore, process conditions such as impeller tip speed can influence

* Corresponding author.

E-mail address: A.Hassanpour@leeds.ac.uk (A. Hassanpour).

<https://doi.org/10.1016/j.cherd.2017.10.038>

0263-8762/© 2017 The Authors. Published by Elsevier B.V. on behalf of Institution of Chemical Engineers. This is an open access article under the CC BY-NC-ND license (<http://creativecommons.org/licenses/by-nc-nd/4.0/>).

the mixing, binder addition and coalescence and/or breakage during granulation process.

A number of researchers investigated the effect of different liquid-binder/solid ratios (Bock and Kraas, 2001; Oulahna et al., 2003; Rahmanian et al., 2009; Realpe and Velázquez, 2008; Saleh et al., 2005) on the granulation process. The role of binder is to form bridges or bonds between the primary particles to form the nuclei and later their coalescence in the granulation process (Mangwandi et al., 2015). It was found that, increasing the liquid/solid ratio leads to an increase in the granule size (Bock and Kraas, 2001; Chitu et al., 2011). In addition, granules produced with high binder viscosity could have a considerably lower strength and wide strength distribution due to poor dispersion of binder on the powder bed (Rahmanian et al., 2011).

Landin et al. (1996) and Betz et al. (2004) have stated that, impeller torque and power consumption values can be used as methods to monitor/follow the granule growth from the initial granule formation phase. Both methods noticeably depend on the cohesive force of the wet mass or the tensile strength of the granules (agglomerates). Furthermore, Sakr et al. (2012) claimed that torque measurement can be used as a reliable control method for monitoring the wetting procedure and scale up, possibly due to the direct relationship of the torque with the mass flow resistance. This information could facilitate selection of a liquid addition range where the granule growth behaviour can be predicted.

The impeller torque profile can be subdivided into three different stages (Leuenberger et al., 2009). In the first stage, a slight increase in torque is usually related to nuclei formation and moisture sorption without the formation of liquid bridges. In the second stage, a rapid/sudden increase in the torque could be due to the attainment of the formation of liquid bridges (pendular). This rapid increase in torque can be correlated with the liquid amount required to achieve the dry binder transition stage. In these conditions, dry binder stickiness promotes a faster granule growth (Cavinato et al., 2010). Finally, a subsequent plateau stage in the torque indicates the transition from the pendular to the funicular state (Leuenberger, 1982). A reliable relationship between power or torque profiles and the saturation degree of the wet mass can be established (Leuenberger, 1982; Leuenberger et al., 1981).

The granulation process in high shear granulators has been investigated at different periods of time, from 2 min (Rahmanian et al., 2011; Realpe and Velázquez, 2008) up to 20 min (Oulahna et al., 2003). The results showed that, increasing the granulation time has a significant effect on granules strength and density, until an optimum time is reached (Rahmanian et al., 2011).

Implementing characterization tools are important for assessing granule qualities and the granulation process. Depending upon whether the assessment is done after or during the process, these tools can be classified as offline and online/inline. In addition, the online tools are more rigorous and accurate and become more critical with the transformation of batch to continuous processing in pharmaceutical applications (Hansuld and Briens, 2014; Suresh et al., 2017).

There are several primary technologies that have been investigated for high-shear wet granulation monitoring. These technologies include power consumption (Hansuld and Briens, 2014; Levin, 2016), near-infrared spectroscopy (Alcalá et al., 2010; Hartung et al., 2011; Liu et al., 2017), Raman spectroscopy (Hansuld and Briens, 2014), capacitance

Table 1 – The properties of the materials.

Properties	α -Lactose	Avicel [®] PH-101	HPMC
Density (kg/m ³)	1543	1555	1315
Aspect ratio mean ^a	0.733	0.598	0.608
BET surface area, m ² /g	0.3478	0.9308	0.4913
Solubility in water (%wt) ^b	21.6	Insoluble	Soluble
D ₁₀ , D ₅₀ and D ₉₀ (microns) ^c	7.8, 40.8 and 123.7	26.1, 71.3 and 156.9	–

^a Based on number distribution.
^b Found from the MSDS sheet of the materials.
^c Malvern 2000S (dry system) based on volume distribution.

measurements (Hansuld and Briens, 2014), microwave measurements (Hansuld and Briens, 2014; Peters et al., 2017), imaging (Kumar et al., 2015; Soppela et al., 2014), focused beam reflectance measurements (Narang et al., 2017), spatial filter velocimetry (Hansuld and Briens, 2014), stress (Hansuld and Briens, 2014), drag flow force (Narang et al., 2016) and vibration measurements (Hansuld and Briens, 2014), as well as acoustic emissions (Hansuld et al., 2012). In addition, advantages, disadvantages and challenges associated with each method for high-shear wet granulation was summarized by Hansuld and Briens (2014). For example, complexity of implementation and measurements, extensive calibration and data reliability as well as the costs are the main disadvantages and challenges of these methods (Hansuld and Briens, 2014; Suresh et al., 2017).

In this work a simple vacuum base online sampling has been used for granulation as no previous work has been reported in this aspect. It is used to study the effect of different parameters and process conditions during the granulation without stopping the process.

2. Materials and methodology

2.1. Materials

A number of commercial powders were used as shown in Table 1. Alpha lactose monohydrate (C₁₂H₂₂O₁₁H₂O) and Avicel PH-101 (microcrystalline cellulose (C₆H₁₀O₅)_n) were used as primary particles and hydroxypropyl methylcellulose (HPMC, C₅₆H₁₀₈O₃₀) was used as the binder. All materials were supplied by Sigma-Aldrich Co., Ltd., UK. Fig. 1 shows the SEM images of both primary powders, where the particles of lactose have a relatively wide size distribution as compared to Avicel. The Micromeritics Tristar 3000 was used to measure the BET Surface Area (m²/g) for the materials. While the density of solids was found using Micromeritics Acupyc 1330 device. Furthermore, particle size, mean aspect ratio, circularity and elongation were measured using the Malvern

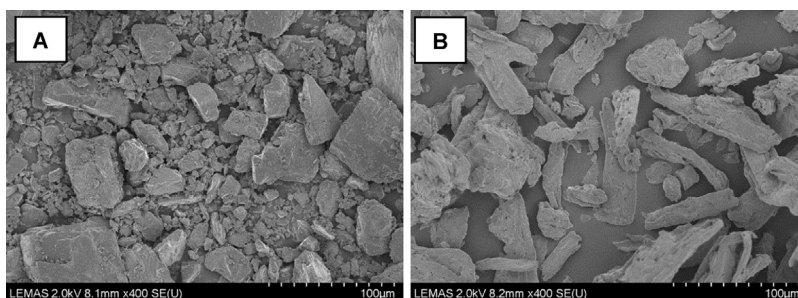


Fig. 1 – SEM images of A) α -lactose monohydrate and B) avicel PH-101 cellulose microcrystalline.

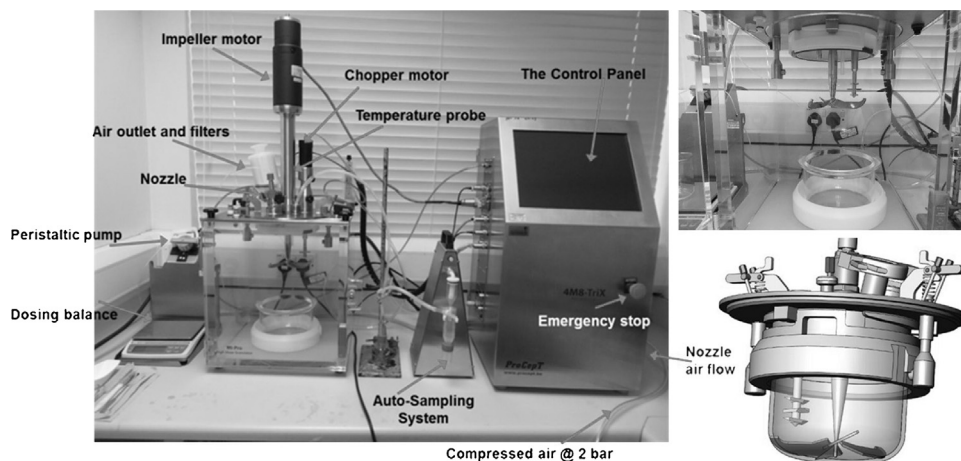


Fig. 2 – Mi-Pro – high shear wet-granulator – ProCepT.

Morphologi G3-S. The Scanning Electron Microscope (HITACHI Benchtop TM3030 Plus) was used to analysis of the sample images.

2.2. Methodology

A number of experiments were carried out to study the granulation process in terms of accuracy and reproducibility for robust results and data. Two sets of experiments were conducted where the effect of impeller speed on impeller torque with and without materials were investigated. For the first experiment the impeller torque vs. different impeller speeds of 30 rpm (0.23 m/s, minimum), 1000 rpm (7.75 m/s) and 1750 rpm (13.56 m/s, maximum) without any materials was recorded. For the second experiment torque was investigated for one impeller speed (1000 rpm) but with two different masses of solid materials (116 and 232 g) and varying volume of added liquid.

Additional experiments were also conducted to investigate the steady state granulation process for a fixed volume of added liquid for the same impeller speed (1000 rpm), where, the liquid addition was stopped at three different points: (i) the starting point of the sudden increase in the torque, (ii) just after the peak point of the torque value and (iii) in between both points.

In this work, a small scale, top driven batch high-shear wet granulator (MiPro, ProCepT, Zelzate, Belgium) was used, as shown in Fig. 2. This granulator comes with two scales (0.5 and 1.9 l), but, in this work, the 1.9 l scale was used. HPMC was used as a solid binder and pre-mixed with the feed materials (Lactose and Avicel). All solid materials were added together into the granulator bowl and mixed for 30 s using impeller speed of 100 rpm. The mass percentage of the formulation for HPMC, Avicel and Lactose, was 5, 30 and 65%, respectively. During the process, the Reverse Osmosis Water (RO-Water) was sprayed on the mixed powders using a Bi-fluid Atomising Nozzle (liquid and air). The RO-Water was pumped using a peristaltic pump (bi-directional, 12 rollers, 100%–160 rpm) and the air was supplied to the system using a compressor (Bambi BB8 SAC). The liquid flow rate is adjusted using the pump speed, while atomizing airflow rate is controlled by a needle valve and both are measured using flow rates sensors within the granulator control panel.

Table 2 shows the process parameters that were used in this work. The liquid/solid ratio can be a function of process

Table 2 – The process parameters for the first set of experiment.

Parameter	Value
Impeller speed	1000 rpm
Chopper speed	3000 rpm
Pump flow rate (water)	3.4 g/min
Air flow rate	3.0 l/min
Bi-fluid nozzle	0.4 mm

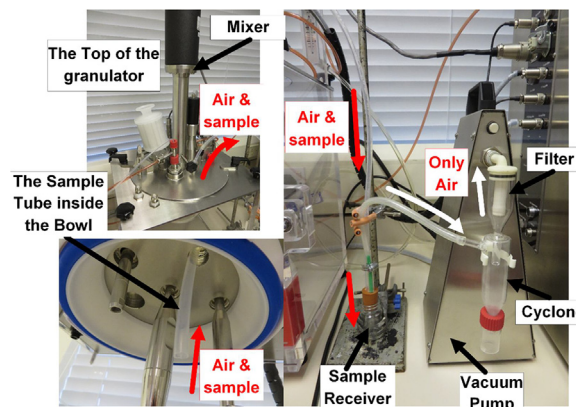


Fig. 3 – The sampling system.

time during the continuous addition as will be presented in the results section.

To study the growth kinetics of the granules during operation (wetting steps), at fixed time intervals, the representative samples of solid were collected from the mixed bed and dried to determine the granule size distribution as a function of processing time. A sampling system was used to take a sample every 2 min during the granulation process. As shown in Fig. 3 the sampling system consists of a small glass cyclone with a filter connected to a vacuum pump. The samples were collected through a tube that is connected to the cyclone inlet, because of the cyclone and the filter the sample can be collected with almost no dust reaching to the vacuum pump.

In addition, for all samples, the final granules were taken immediately after the end of the process time intervals and dried. To minimize incidental alteration in particle size distribution due to drying method (e.g. attrition in fluid bed dryer,

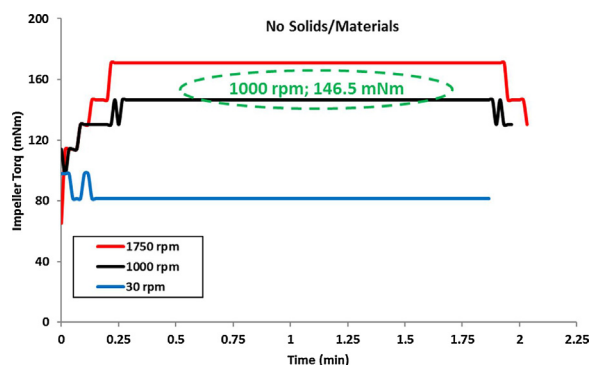


Fig. 4 – The torque profiles for the three-different impeller speed without any materials: 30 rpm (0.23 m/s, minimum), 1000 rpm (7.75 m/s; desired) and 1750 rpm (13.56 m/s, maximum).

caking in oven at high temperature) the drying was gently performed in an oven for around 12 h with temperature and pressure of 35 °C and 1 atm, respectively. After that, the SEM was used to analysis the samples images. The weight of the collected samples during the process time was between 4 and 6 g. The maximum number of collected samples was 9 samples per run. Therefore, the total material removed from the mixture during the granulation process was around 45 g (out of 274 g total weight), which is about 14% of the total mixture.

3. Results and discussion

The impeller torque profile was recorded continuously and was used as a guide to monitor the granule formation in the granulation processes. Fig. 4 shows the torque profile without any materials for three different impeller speeds: 30, 1000 and 1750 rpm (the minimum, the desired and the maximum speed, respectively). These experiments were run three times (for each) to test repeatability and reliability of the results. The average standard deviation was found to be less than $\pm 0.03\%$, which cannot be shown in the figure as error bars are very small. Generally, increasing the impeller speed leads to an increase in the impeller torque. Based on these results for this granulator type, increasing the impeller speed from 30 to 1750 rpm leads to an increase in the torque by 2.1 times in the absence of any material. The torque value is 146.5 mNm for the impeller speed of 1000 rpm as shown in Figs. 4 and 5.

Fig. 5 shows the impeller torque profile without and with solid materials (116 and 232 g with the same liquid addition rate) using 1000 rpm impeller speed. Increasing the materials from zero to 232 g increases the impeller torque value by 1.8 times. The torque profiles for the second scenario (with materials) of the granulation experiments showed similar trends with time, as noted and reported by a number of authors (Betz et al., 2004; Cavinato et al., 2010; Landin et al., 1996). As shown in Fig. 5, a slight increase in the impeller torque value at the beginning (from time 0 to 8 min) of the process has often been recognized, which is possibly due to the progressive spread of the liquid. Then, a more significant increase in the profile slope is observed (from time 8 to 10 min), presumably due to the wetting process of solid mass. After this initial stage, impeller torque profiles show a sudden increase (from time 10 to 12.5 min). A number of authors explained this phenomenon by considering the initial formation of liquid bridges between particles, thus leading to the achievement of the pendular

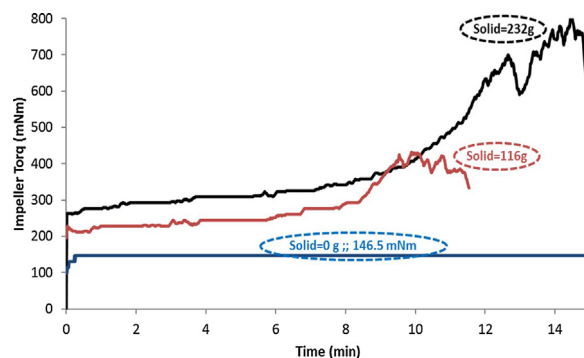


Fig. 5 – Comparison between three different impeller torque profiles for (zero, 116 and 232 g of materials) using 1000 rpm, based on the process time (min).

state. In addition, two more stages for the torque profile can be added, which are the peak (at 12.5 min) and the short sudden drop after that point (from time 12.5 to 13 min). The peak shows the optimum volume of liquid that can be added to the system to form granules, where the adhesive force reaches the maximum and leads to an increase the torque. In addition, the sudden drop is related to the formation of the granules. After that, increasing the liquid ratio leads to the production of larger granules size until it reaches to the production of over wetted paste type material. It should be noted in these experiments, same amount of water has been added by time (water flow rate) for two different masses of solid materials, hence the peak torque values for the two experiments occur at different times. Different volumes of materials (116 and 232 g) obviously require different amounts of liquid (24 and about 47 ml, respectively) for the sudden increase and the peak in the torque profiles, as noticed by other researchers (Cavinato et al., 2010).

The relationship between the impeller torque value and the liquid addition (at different process times) was investigated for the case with 232 g of solid materials, as shown in Fig. 6A and B. It should be noted that the variation regarding the continuous removal of materials was taken into account with the liquid/solid percentage calculation. This experiment was repeated four times to test repeatability and reliability of the data. Fig. 6A shows the relationship between the gradient of impeller torque profile and liquid/solid percentage for the four runs with the liquid/solid percentage. In addition, the difference between torque values from various runs is shown in Fig. 6B. A good agreement between the four runs for the first 10 min (point A) can be observed, however, later there is a more noticeable fluctuation on the torque value where the granules have reached the intermediate step in their size changes. Overall, Fig. 6A and B suggest that, the experiment is fairly repeatable and reproducible. For further investigations of the sudden increase regions of the torque profile, three points (A, B and C) were chosen, as shown in Fig. 6A and B. The liquid amount required to cause the sudden increase in the torque value (identified as point A) has been used as a reference point to describe the first stage of the agglomeration process and the achievement of the pendular state. Similarly, the maximum amount of liquid required to form granules can be found from the peak (point C) in the torque profile, as shown in Fig. 6A and B. However, point B was selected to investigate the granules behaviour in between the starting and the end of the granule formation stage.

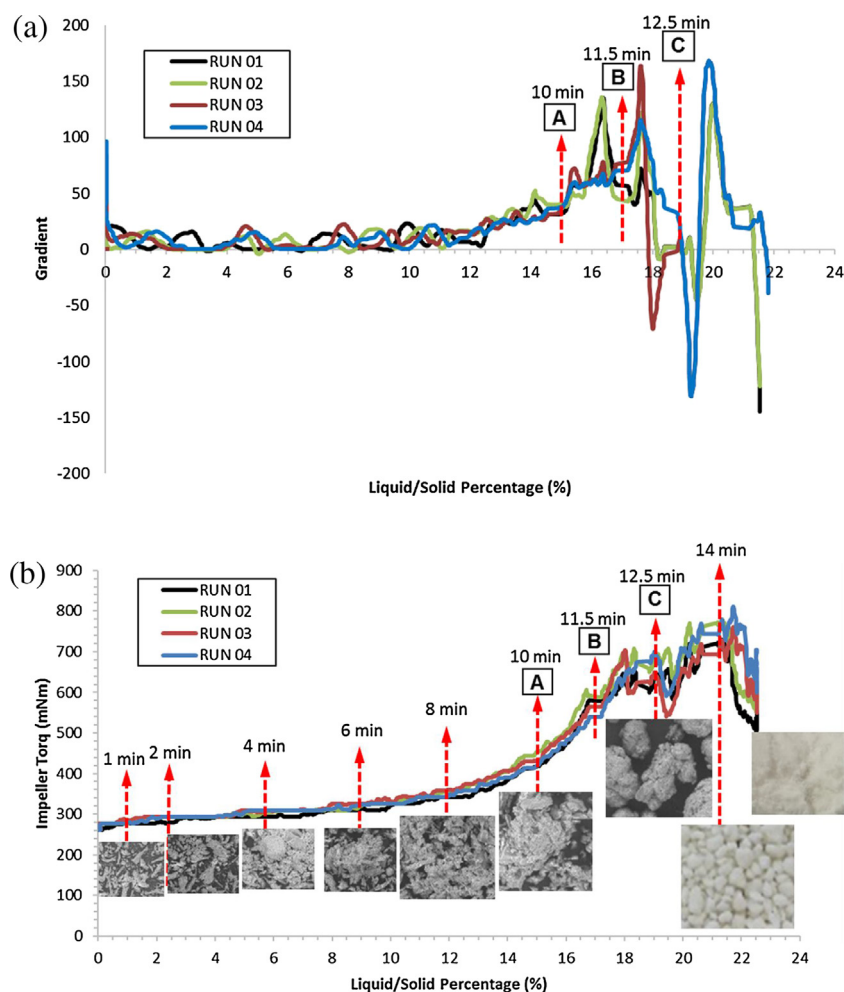


Fig. 6 – (A) The relationship between the gradient of the impeller torque and the liquid/solid percentage vs. the liquid/solid addition percentage for the 232 g of materials. Different colours represent repeated identical runs. A, B and C indicate the three chosen points for the steady state investigation. (B) The relationship between the torque vs. the liquid/solid addition percentage for the 232 g of materials. Different colours represent repeated identical runs. Sampling time is indicated by the arrows, and the letters indicate the three chosen points for the steady state investigation.

Fig. 7A shows the SEM images of the granules acquired during wetting stages using the sampling system at different process times (1, 2, 4, 6, 8, 10, 12.5, 14 and 16 min). Under these conditions, nucleation stage was found to be after the first 2 min and then granules started to grow. SEM images of original samples (at 0 min) and samples at 1 and 2 min (labelled as wetting and nucleation stages), are shown in Fig. 7B. The difference between the images at 0, 1 and 2 min confirms the nucleation has started after the second minute at 2.5% liquid addition. After 10 min, the granules (100–300 μm) were formed. Increasing the liquid addition after that leads to the oversized granules until the torque value reaches its peak. However, increasing the liquid binder ratio further leads to the over-wetted materials (paste type).

It is worth noting that the sampling suction vacuum was measured using a manometer (Fisherbrand™ Traceable™ Pressure/Vacuum Gauges) as 45 mbar and the air flow rate was measured using an air flow meter (Cole Parmer) as 4 l/min. The air velocity was then calculated to be 0.85 m/s. There is no obstacle on the way and particles do not impact to any object. Therefore, the sampling system should not damage the granules. This dynamic sampling technology allows facile detection of the end point of granulation, e.g. the granula-

tion time and the required liquid volume are being readily obtained for different material ratios and operational conditions as shown in Fig. 6.

Further experiments were carried out to investigate the steady state conditions for granulation for fixed added liquid. In this case, the liquid addition was stopped at different points (A–C as shown in Fig. 6). Therefore, total added liquid for case A, B and C are 38 ml, 41 ml and 45 ml, respectively. Fig. 8 shows the trend of torque when the liquid addition was stopped at three points A, B and C. From case C, it can be seen that, there is a sudden drop in torque and after nearly 2 min the torque value decreases with a very low slope by time. However, the temperature inside the granulator bowl increases with time and reaches as high as 43 °C. As there is no further liquid addition, the granules drying process can take place at temperature higher than the ambient conditions inside the granulator. In addition, the granules mass gradually decreases with time as liquid evaporation takes place that leads to a slight reduction in the impeller torque. Similar trends were observed for the case A and B as shown in Fig. 8.

Fig. 9 shows the full particle size distribution of the three cases (A, B and C at 10.5, 11.4 and 12.5 min, respectively) compared to the original mixed materials (at time 0 min and no

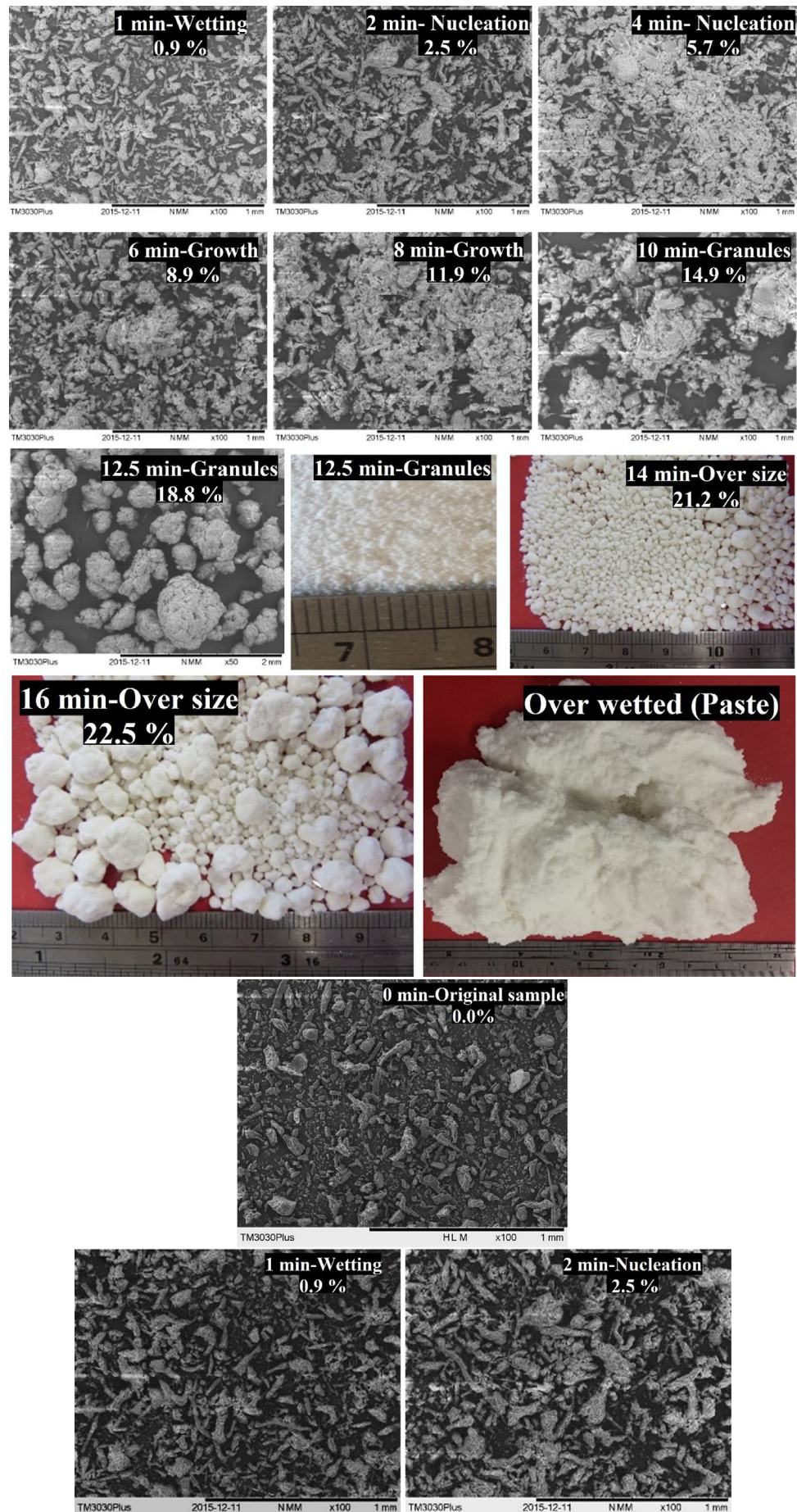


Fig. 7 – (A) Granules size based on process time and different liquid/solid percentages. (B) SEM images of powders mixture at initial experimental time (0, 1 and 2 min) for 0.0, 0.9 and 2.5% liquid/solid ratios, respectively, referring to free powder (original sample), initial nucleation and nucleation.

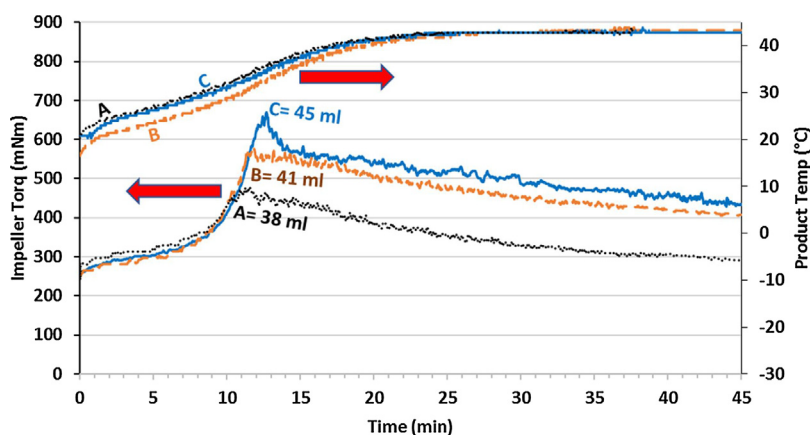


Fig. 8 – The impeller torque and granule temperature profiles against the process time for the steady state experiment using 232 g of solid materials for the three points at A = 38 ml, 10.5 min, B = 41 ml, 11.5 min and C = 45 ml, 12.5 min.

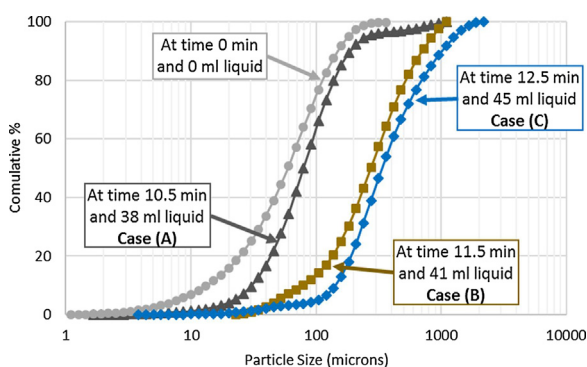


Fig. 9 – Particle size distribution of the three cases (A–C) compared to the original mixed materials (at time 0 min and no liquid addition), results volume based, Malvern-2000 dry system was used.

liquid addition). It can be seen that the particles have been enlarged significantly (6 times larger) by adding 45 ml of water. Adding 38 ml of water to powders to point A results in 50% increase in average particles size. Further 3 ml of water addition (from 38 ml in case A to 41 ml in case B) increases average particle size by more than 3 times at point B. Finally from point B to point C, extra 4 ml of water addition (from 41 ml to 45 ml in case C) leads to 25% increase in d_{50} and d_{90} of granules. That is because the granules have gained the optimal liquid ratio to for further growth without excessive liquid addition to the end of the process.

SEM images of the sampled granules were taken when the liquid addition was stopped for different cases (A, B and C) as shown in Figs. 10 and 11. The SEM images refer to granules evolution at different times for individual cases. Fig. 10 shows that for case A two types of granules (consolidated and partially formed) can be formed where the liquid addition percentage is fixed at 14%. It can be seen that the consolidated granules survive as the time progressed. However, partially formed granules disintegrate to their primary particles towards the end of process, presumably as there is not enough liquid to further bind partially formed granules.

Fig. 11 shows the SEM images of both cases B and C. For the case B, partially formed granules seem to be able to survive towards the end of process by further consolidation, but leading to smaller sized granules as compared to the fully evolved

granules. However, it can be seen that for case C, most of the granules have been already formed and consolidated. At the end of the process, there is a slight change on the surface of the granules that becomes smoother as shown in Fig. 11B. Overall, it can be concluded that larger granules (200–1200 μm) form for the case C (where liquid addition is fixed at 45 ml) as compared to case B (100–700 μm). However, for the case A, most of the partially formed granules will not survive the process as there is not enough liquid for binding them further together.

By comparing full size distribution and SEM images it can be seen that particle size ranges reasonably agree and the sampling system in this work can provide a representative particle size, perhaps due to the fact that it can take sample in-process from a mixed dynamic mass. The sampling method developed in this work allows researcher/formulators to understand and follow the wetting stages and formation of granule structure step by step and obtain information on the granulation time and the required liquid volume for various formulations and operational conditions.

4. Conclusions

The growth kinetics of the granules during operation for a high shear mixer granulator for continuous as well as fixed liquid addition was investigated. A sampling system was used to take samples at fixed times during the granulation process. The results showed that the nucleation stage occurs in the first 2 min then followed by the growth stage up to 8 min. The granules start to form after 10 min and their size will increase by further liquid addition. Furthermore, for the cases of fixed liquid addition, the final particle size distribution depends on the point where the liquid addition was stopped (i.e. fixed amount of added liquid). When liquid amount was fixed at 38 ml there was no change on the size of the totally formed granules, while the partially formed granules disintegrated to their primary particles towards the end of process, presumably as there was not enough liquid to further bind partially formed granules. However, when the liquid addition was fixed at 45 ml, totally formed granules were smoothed and became more rounded as the processing time extended further.

The method presented in this paper can facilitate an online determination of the granulation time and the required liquid volume for material formulation and operational conditions.

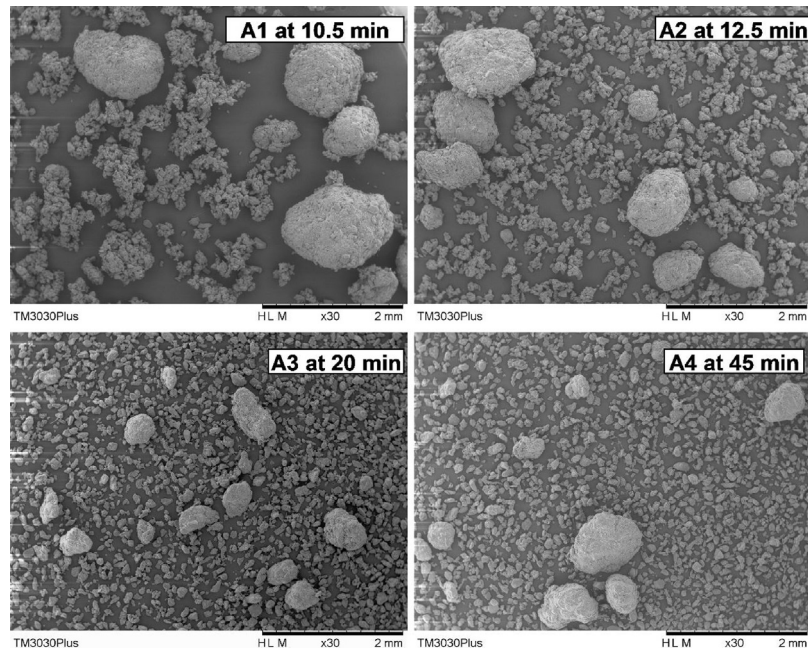


Fig. 10 – SEM images of granules for the steady state (continuous) of case A (at 10.5 min); for four process times at 10.5, 12.5, 20 and 45 min (end of process time).

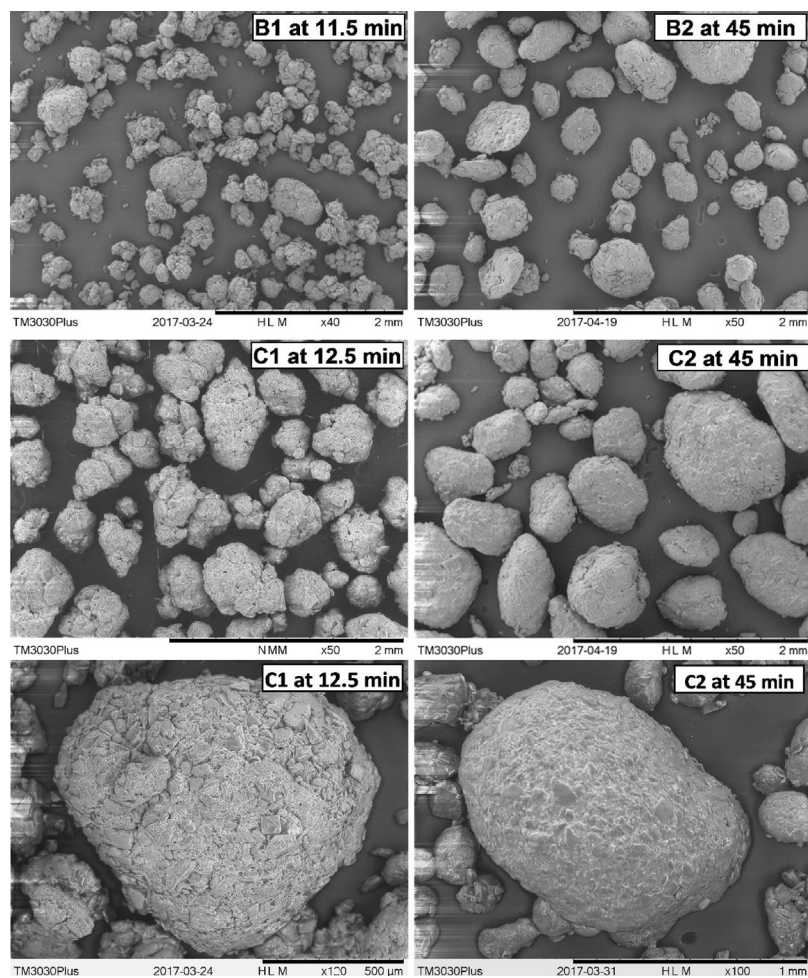


Fig. 11 – The granules SEM images for the steady state of two different cases: at the desired point (11.5 and 12.5 min) and the end of process point (45 min), and the SEM images with higher magnitude to show the smoothness of a granule with process time for case C at 12.5 and 45 min.

Acknowledgement

This project has received funding from the European Union's Horizon 2020 research and innovation programme under grant agreement No. 637232.

References

- Alcalà, M., Blanco, M., Bautista, M., González, J.M., 2010. On-line monitoring of a granulation process by NIR spectroscopy. *J. Pharm. Sci.* 99, 336–345.
- Augsburger, L.L., Vuppala, M.K., 1997. Theory of granulation. In: Parikh, D.M. (Ed.), *Handbook of Pharmaceutical Granulation Technology*. Marcel-Dekker, New York, pp. 7–23.
- Betz, G., Bürgin, P.J., Leuenberger, H., 2004. Power consumption measurement and temperature recording during granulation. *Int. J. Pharm.* 272, 137–149.
- Bock, T.K., Kraas, U., 2001. Experience with the Diosna mini-granulator and assessment of process scalability. *Eur. J. Pharm. Biopharm.* 52, 297–303.
- Cavinato, M., Bresciani, M., Machin, M., Bellazzi, G., Canu, P., Santomaso, A.C., 2010. Formulation design for optimal high-shear wet granulation using on-line torque measurements. *Int. J. Pharm.* 387, 48–55.
- Chitu, T.M., Oulahna, D., Hemati, M., 2011. Wet granulation in laboratory scale high shear mixers: effect of binder properties. *Powder Technol.* 206, 25–33.
- Farber, L., Tardos, G., Michaels, J.N., 2003. Use of X-ray tomography to study the porosity and morphology of granules. *Powder Technol.* 132, 57–63.
- Garboczi, E.J., 2002. Three-dimensional mathematical analysis of particle shape using X-ray tomography and spherical harmonics: application to aggregates used in concrete. *Cem. Concr. Res.* 32, 1621–1638.
- Hancock, B.C., Mullarney, M.P., 2005. X-ray micro-tomography of solid dosage forms. *Pharm. Technol.* 29, 92–100.
- Hansuld, E.M., Briens, L., 2014. A review of monitoring methods for pharmaceutical wet granulation. *Int. J. Pharm.* 472, 192–201.
- Hansuld, E.M., Briens, L., Sayani, A., McCann, J.A.B., 2012. Monitoring quality attributes for high-shear wet granulation with audible acoustic emissions. *Powder Technol.* 215, 117–123.
- Hartung, A., Knoell, M., Schmidt, U., Langguth, P., 2011. Role of continuous moisture profile monitoring by inline NIR spectroscopy during fluid bed granulation of an Enalapril formulation. *Drug Dev. Ind. Pharm.* 37, 274–280.
- Hemati, M., Benali, M., 2007. Chapter 8. In: Bröckel, U., Meier, W., Wagner, G. (Eds.), *Product Design and Engineering: Best Practices*. Wiley-VCH Verlag GmbH & co. KGaA, Weinheim.
- Iveson, S.M., Litster, J.D., Hapgood, K., Ennis, B.J., 2001. Nucleation, growth and breakage phenomena in agitated wet granulation processes: a review. *Granulation Coat. Fine Powders* 117, 3–39.
- Klobes, P., Riesemeier, H., Meyer, K., Goebels, J., Hellmuth, K.H., 1997. Rock porosity determination by combination of X-ray computerized tomography with mercury porosimetry. *Fresenius' J. Anal. Chem.* 357, 543–547.
- Kumar, A., Dhondt, J., De Leersnyder, F., Vercruyssen, J., Vanhoorne, V., Vervaet, C., Remon, J.P., Gernaey, K.V., De Beer, T., Nopens, I., 2015. Evaluation of an in-line particle imaging tool for monitoring twin-screw granulation performance. *Powder Technol.* 285, 80–87.
- Landin, M., York, P., Cliff, M.J., Rowe, R.C., Wigmore, A.J., 1996. Scale-up of a pharmaceutical granulation in fixed bowl mixer-granulators. *Int. J. Pharm.* 133, 127–131.
- Leuenberger, H., 1982. Granulation, new techniques. *Pharm. Acta Helv.* 57, 72–82.
- Leuenberger, H., Bier, H.P., Sucker, H., 1981. Determination of the liquid requirement for a conventional granulation process. *German Chem. Eng.* 4, 13–18.
- Leuenberger, H., Puchkov, M., Krausbauer, E., Betz, G., 2009. Manufacturing pharmaceutical granules: is the granulation end-point a myth? *Powder Technol.* 189, 141–148.
- Levin, M., 2016. Chapter 3—Wet Granulation, How to Scale-Up a Wet Granulation End Point Scientifically. Academic Press, Boston, pp. 19–42.
- Liu, R., Li, L., Yin, W., Xu, D., Zang, H., 2017. Near-infrared spectroscopy monitoring and control of the fluidized bed granulation and coating processes—a review. *Int. J. Pharm.* 530, 308–315.
- Lowell, S., Shields, J.E., Thomas, M.A., Thommes, M., 2012. *Characterization of Porous Solids and Powders: Surface Area, Pore Size and Density*. Springer, Netherlands.
- Mangwandi, C., JiangTao, L., Albadarin, A.B., Dhenge, R.M., Walker, G.M., 2015. High shear granulation of binary mixtures: effect of powder composition on granule properties. *Powder Technol. B* 270, 424–434.
- Narang, A.S., Sheverev, V., Freeman, T., Both, D., Stepaniuk, V., Delancy, M., Millington-Smith, D., Macias, K., Subramanian, G., 2016. Process analytical technology for high shear wet granulation: wet mass consistency reported by in-line drag flow force sensor is consistent with powder rheology measured by at-line FT4 powder Rheometer®. *J. Pharm. Sci.* 105, 182–187.
- Narang, A.S., Stevens, T., Macias, K., Paruchuri, S., Gao, Z., Badawy, S., 2017. Application of in-line focused beam reflectance measurement to Brivanib alaninate wet granulation process to enable scale-up and attribute-based monitoring and control strategies. *J. Pharm. Sci.* 106, 224–233.
- Oulahna, D., Cordier, F., Galet, L., Dodds, J.A., 2003. Wet granulation: the effect of shear on granule properties. *Powder Technol.* 130, 238–246.
- Peters, J., Bartscher, K., Döscher, C., Taute, W., Höft, M., Knöchel, R., Breitzkreutz, J., 2017. In-line moisture monitoring in fluidized bed granulation using a novel multi-resonance microwave sensor. *Talanta* 170, 369–376.
- Rahmanian, N., Ghadiri, M., Jia, X., Stepanek, F., 2009. Characterisation of granule structure and strength made in a high shear granulator. *Powder Technol.* 192, 184–194.
- Rahmanian, N., Naji, A., Ghadiri, M., 2011. Effects of process parameters on granules properties produced in a high shear granulator. Special issue on agglomeration. *J. Urol.* 89, 512–518.
- Realpe, A., Velázquez, C., 2008. Growth kinetics and mechanism of wet granulation in a laboratory-scale high shear mixer: effect of initial polydispersity of particle size. *Chem. Eng. Sci.* 63, 1602–1611.
- Sakr, W.F., Ibrahim, M.A., Alanazi, F.K., Sakr, A.A., 2012. Upgrading wet granulation monitoring from hand squeeze test to mixing torque rheometry. *Saudi Pharm. J.* 20, 9–19.
- Saleh, K., Vialatte, L., Guigon, P., 2005. Wet granulation in a batch high shear mixer. Granulation Across the Length Scales—2nd International Workshop on Granulation 60, 3763–3775.
- Soppela, I., Antikainen, O., Sandler, N., Yliruusi, J., 2014. On-line monitoring of fluid bed granulation by photometric imaging. *Eur. J. Pharm. Biopharm.* 88, 879–885.
- Stanley-Wood, N.G., Shubair, M.S., 1979. The influence of binder concentration on the intra- and intergranular porosity of pharmaceutical granules. *Powder Technol.* 22, 153–160.
- Suresh, P., Sreedhar, I., Vaidhiswaran, R., Venugopal, A., 2017. A comprehensive review on process and engineering aspects of pharmaceutical wet granulation. *Chem. Eng. J.* 328, 785–815.
- Tardos, G.I., Khan, M.I., Mort, P.R., 1997. Critical parameters and limiting conditions in binder granulation of fine powders. *Powder Technol.* 94, 245–258.